Journal of Advanced Research in Natural and Applied Sciences
dergipark.org.tr/en/pub/jarnas
Open Access

ISSN: 2757-5195 11 (2) (2025) 187-196 doi.org/10.28979/jarnas.1666819

# Design and Evaluation of Nanoparticle-Reinforced Glass for Radiation Shielding in Angiography: An MCNP Simulation Study

Navid Kheradmand[1], Mustafa Çağlar[2]

**Article Info**
*Received*: 27 Mar 2025
*Accepted*: 03 Jun 2025
*Published*: 30 Jun 2025
Research Article

**Abstract** − Angiography is a widely utilized diagnostic and treatment method involving relatively high radiation doses for patients and personnel. Protecting radiation-sensitive organs, such as the eye lens, is crucial in this imaging modality. In this study, we employed the Monte Carlo N-Particle Transport (MCNP) code to design transparent shields incorporating metal nanoparticles (NPs). Two types of phosphate glass—one with lead and one with bismuth—were designed and simulated. ZnO-$Bi_2O_3$-$P_2O_3$ and ZnO-PbO-$P_2O_3$ were analyzed at six concentrations (0, 10, 20, 30, 40, 50 wt%). We calculated the linear attenuation coefficients, mass attenuation coefficients, and half-value layer for each sample across eight photon energies (50, 60, 80, 100, 120, 140, 150, and 200 kV), which are primarily used in angiography. A good agreement was observed between the simulated results and those from the XCOM database. The maximum mass attenuation coefficients were found for the PZBi 50 glass sample. The results suggest that the MCNP code can be a reliable alternative to experimental methods for other glass materials and systems, calculated for their photon attenuation characteristics. Among the studied samples, Bi-doped glasses demonstrated slightly better attenuation properties than Pb-doped ones, especially at lower photon energies. This superiority is mainly attributed to the higher atomic number of Bi and its enhanced photoelectric interaction probability. While the consistency between MCNP and XCom results reinforces the credibility of the simulation approach.

**Keywords** − *Monte Carlo simulation, angiography, glass shields, radiation shields, radiation protection*

## 1. Introduction

The increase in the use of ionising radiation in X-ray machines, particularly in angiography, is becoming more common for diagnosing a range of medical conditions. Currently, over ten million diagnostic radiology procedures involving ionizing radiation are performed daily worldwide, resulting in heightened radiation exposure for patients [1]. This increased exposure poses significant risks, especially to sensitive organs such as the lens, thyroid gland, and breast, which can elevate the risk of radiation-induced effects, including cancer [2]. This situation highlights the urgent need for effective protection against high-energy X-rays using non-toxic shielding materials [3]. Historically, lead has been the first choice for radiation shielding due to its high atomic number, effectively blocking ionizing radiation. However, lead has significant drawbacks. These include its inflexibility, excessive weight, toxicity, and limited mechanical and chemical stability [4]. Consequently, researchers are investigating alternative materials to enhance radiation protection. In this

[1]navid.kheradmand@medipol.edu.tr; [2]drmustafacaglar@gmail.com (Corresponding Author)
[1]Department of Health Physics, Graduate School of Health Sciences, İstanbul Medipol University, İstanbul, Türkiye
[1,2]Department of Radiotherapy, Vocational School of Health Services, İstanbul Medipol University, İstanbul, Türkiye

context, glass has emerged as a promising option because it is transparent to visible light, easy to fabricate, and can be modified through various compositional methods to improve its shielding effectiveness [5].

Researchers are developing protective glasses that incorporate nanoparticles (NPs) of bismuth (Bi), Lead (Pb), barium (Ba), and tungsten (W) [6, 7]. These materials, known for their high atomic numbers and beneficial properties such as flexibility, non-toxicity, and lightweight nature, enhance the glasses effectiveness in shielding against ionizing radiation. This innovative approach aims to improve safety for individuals exposed to radiation and opens new possibilities for protective gear in medical and industrial applications [8]. To optimize these materials, numerical modeling, especially through Monte Carlo (MC) simulations like Geant4 and MCNP, is used to assess their performance against X-rays and gamma rays [9].

For instance, in a study by Çağlar et al. [10], a glassy structured sodium silicate (Na2Si3O7) matrix was examined, with the presence of micro-sized and nano-sized silver (Ag) particles at varying weight percentages, to provide an example of the type of research that can be conducted. The findings revealed that adding NPs significantly enhances radiation shielding effectiveness compared to micro-sized particles, particularly at lower concentrations and photon energies. Studies have consistently shown that NPs, due to their larger surface-area-to-volume ratio, provide superior photon absorption capabilities [11]. For example, studies on Bi and gadolinium oxide (Gd2O3) NPs have demonstrated that nano-sized composites outperform their micro counterparts in shielding X-rays or gamma rays by approximately 28% [3]. In a separate study, Zaid et al. [12] conducted a theoretical analysis using XCom software to evaluate the radiation shielding effectiveness of Bi2O3–TiO2–V2O5–Na2O–TeO2 glasses designed to provide gamma-ray shielding. The glass composition containing Bi2O3 at 20% wt demonstrated the most effective gamma-ray shielding. In a different study, experimental and theoretical methods were used to determine the gamma-ray attenuation properties of metal oxide-doped glasses within a photon energy range of 53–383 keV. It was established that the sample of glass containing the highest concentration of heavy metals, which was found to consist of 5.05% Bi2O3, 5.05% MnO2, 4.5% ZnO, 1.7% Al2O3, and 67.65% SiO2, exhibited the optimal gamma shielding capacity [13].

In addition, Kebaili et al. [14] performed an MC simulation to investigate the radiation shielding performance of alkaliborate glasses with the substitution xTiO2/(10-x) V2O5 (referred to as LBZ-TV glasses), where x values ranged from 0 to 10%. They found that the LBZ-TV glasses developed in their study exhibited superior radiation shielding performance compared to conventional materials, including standard ordinary and barite concretes and lead-free glasses. In another study, Won-in et al. [15], utilizing Ba NPs, resulted in Pb-free radiation shielding glass fabrication. In the present study, the researchers fabricated lead-free glass specimens utilizing 40% by weight of local quartz sand, along with varying concentrations of $BaCO_3$ (20-40% by weight) as the base material. This experimental approach was employed for the purpose of examining the gamma attenuation characteristics at 662 keV. They suggested that a denser Pb-free glass with a high refractive index can improve attenuation properties, making it a viable alternative to lead for gamma-ray protection.

Given that, numerous studies have investigated protective materials against ionizing radiation, each highlighting unique advantages and disadvantages. While much research has focused on the effectiveness of various materials, there has been limited discussion on the role of NPs when combined with glass base materials to enhance radiation protection [16]. This gap underscores the need to further explore the protective capabilities of glasses reinforced with NPs, as these composites may offer improved shielding properties. Recent developments indicate that incorporating high atomic number NPs such as Bi and Pb into composite materials can significantly enhance their effectiveness against ionizing radiation. In this context, we evaluated the radiation shielding properties of glasses reinforced with NPs of Bi and Pb using MCNP simulation techniques. This research is particularly relevant in medical imaging, nuclear safety, and materials science, where effective radiation shielding is crucial for ensuring safety and efficacy. This study evaluates the radiation shielding performance of Bi- and Pb-doped phosphate glasses using MCNPX simulations. The aim is to support safer and more effective shielding solutions in medical imaging, particularly in angiography.

## 2. Materials and Methods

The current study is a fundamental and applied investigation utilizing the MCNP simulation code. Initially, research focused on various types of glasses and the potential for incorporating non-lead materials. Following preliminary studies, two glass types were selected for further examination: phosphate glass and normal glass. The study aimed to simulate and compare the radiation attenuation capabilities of these lead-free glasses when heavy non-lead materials were added.

### 2.1 Phosphate Glasses

This study designed and simulated two types of phosphate glass: one incorporating lead and bismuth, and the other without these materials. The specific compositions included $ZnO$-$Bi_2O_3$-$P_2O_3$ and $ZnO$-$PbO$-$P_2O_3$ glasses, which were examined at six varying concentrations (0, 10, 20, 30, 40, 50 wt%). The objective was to calculate each sample's linear and mass attenuation coefficients across eight photon energies (50, 60, 80, 100, 120, 140, 150, and 200 keV). Simulations were conducted at three different thicknesses for each energy level to achieve this. The mass attenuation coefficient was derived from the transmitted photon flux using the Beer-Lambert relation. The reduction coefficients related to these thicknesses were obtained to determine the mass attenuation coefficient using the Beer-Lambert relation. This theory postulates a correlation between the phenomenon of light absorption and the properties of the medium through which the light travels. Table 1 presents the physical characteristics of six types of bismuth-doped phosphate glass ($ZnO$-$Bi_2O_3$-$P_2O_3$) that were simulated.

**Table 1.** Physical characteristics and percentage of $ZnO$-$Bi_2O_3$-$P_2O_3$ phosphate glass components.

| Sample | Element (wt%) | | | Density |
|---|---|---|---|---|
| | ZnO | $Bi_2O_3$ | $P_2O_3$ | (g/cm$^3$) |
| PZBi0 | 50 | 0 | 50 | 0.3126 |
| PZBi10 | 40 | 10 | 50 | 0.3087 |
| PZBi20 | 30 | 20 | 50 | 0.2984 |
| PZBi30 | 20 | 30 | 50 | 0.2891 |
| PZBi40 | 10 | 40 | 50 | 0.2798 |
| PZBi50 | 0 | 50 | 50 | 0.2703 |

Similarly, Table 2 displays the physical characteristics of six types of phosphate glass with the presence of lead nanoparticles ($ZnO$-$PbO$-$P_2O_3$) that were also simulated.

**Table 2.** Physical characteristics and percentage of $ZnO$-$PbO$-$P_2O_3$ phosphate glass components.

| Sample | Element (wt%) | | | Density |
|---|---|---|---|---|
| | ZnO | PbO | $P_2O_3$ | (g/cm$^3$) |
| PZPb0 | 50 | 0 | 50 | 3.177 |
| PZPb10 | 40 | 10 | 50 | 3.493 |
| PZPb20 | 30 | 20 | 50 | 4.121 |
| PZPb30 | 20 | 30 | 50 | 4.419 |
| PZPb40 | 10 | 40 | 50 | 4.802 |
| PZPb50 | 0 | 50 | 50 | 4.845 |

### 2.2 Theoretical Background

When X-rays of suitable energy traverse matter, they undergo attenuation through various interactions. The following phenomena are to be considered: the photoelectric effect (PE), Compton scattering (CS), and pair production (PP). These processes result in an exponential decrease in radiation intensity, which is influenced by the thickness of the absorbing material. This relationship is mathematically described by Beer-Lambert law, represented by (2.1):

$$I = I_0 e^{-\mu x} \quad (2.1)$$

The parameters of relevance in this context are $I_0$ and I, representing the incident and transmitted X-ray intensities, respectively. To establish a comprehensive model of the process, it is necessary to include x, representing the absorbing medium's thickness. The fifth parameter required to establish a full process model is μ ($cm^{-1}$). This is known as the linear attenuation coefficient, and it is one of the most significant shielding parameters, the significance of which depends on the X-ray energy and the absorber composition. To remove the dependence of the attenuation coefficient (μ) on material density, the mass attenuation coefficient (μm = μ/ρ) is utilized, where ρ represents the density of the material.

In the present study, the MCNP and the XCom database have been used for modeling the radiation interaction of photons with material and the transportation with material. The difference between μm values of the methods (MCNP, XCom) is achieved from the following (2.2):

$$Diff\ (\%) = \left|\frac{\mu_1 - \mu_2}{\mu_1}\right| 100 \quad (2.2)$$

## 2.3 MCNP Code

This study employed the MC N-particle transport code MCNP version 2.6.0, developed at Los Alamos National Laboratory (LANL) in New Mexico. MCNP is a comprehensive code designed for transporting neutrons, photons, and electrons, allowing for simulations that combine these particle types. The input parameters for MCNP were carefully defined in the input files, detailing cell cards, material cards, surface cards, and energy source features. The simulation geometry was set up within a cylindrical space measuring 100 centimeters in height and 30 centimeters in diameter. A surface source with a diameter of 5 millimeters was specified using commands such as PAR, POS, ERG, RAD, AXS, VEC, and DIR. Additionally, lattice (LAT) and universe (U) cards were used to define the matrix and filler materials (Figure 1). To determine the μm for all samples, monoenergetic beams in the 60-200 keV energy range were simulated. This range was chosen for its significance in future experimental studies on X-ray machines commonly utilized in diagnostic radiology laboratories. The findings from these simulations will enhance our understanding of how different glass compositions attenuate ionizing radiation effectively.

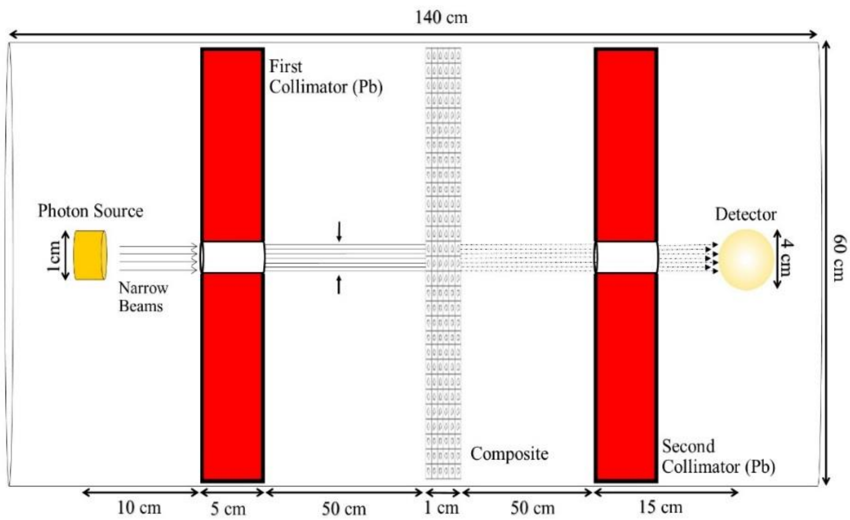


**Figure 1.** Representation of the geometry simulated in Monte Carlo software (no scale).

## 2.4 XCom Standard Database

The XCom database is essential for calculating photon cross-section data, specifically for interactions involving X-rays and gamma rays with various materials. Developed by the National Institute of Standards and Technology (NIST), XCom offers a comprehensive range of data, including partial and total cross sections, mass attenuation coefficients, and effective atomic numbers. It encompasses a range of interaction processes, including coherent and incoherent scattering, pair production, and photoelectric absorption. The energy range covered spans from 1 keV to 100 GeV. In this study, we utilized the XCom program in comparison with MCNP simulations.

## 2.5 Validation of MC Models Through XCom Database Comparison

The accuracy and reliability of the MC models were evaluated by comparing simulation results with data from the XCom database, focusing on a standard lead shield. This comparison ensured that the MC models accurately reflect real-world radiation interactions with shielding materials. Linear attenuation coefficients for lead were calculated from the MC simulations and compared to XCom reference values, allowing for a detailed analysis of discrepancies. Once the simulations were validated, the input codes were used to calculate mass attenuation coefficients for various samples, enhancing our understanding of material effectiveness in radiation protection.

## 3. Results and Discussion

## 3.1. Verification of Advanced Code

To verify the accuracy of the simulation code, we compared the results obtained from our code with data from the Xcom standard database. As illustrated in Figure 2, there is a strong correlation between the two datasets, confirming the reliability of the developed code. Figure 2(A) depicts the results for bismuth metal, while Figure 2(B) illustrates the shielding properties of pure silicon. This validation ensures that our simulation accurately reflects real-world radiation interactions with various materials.

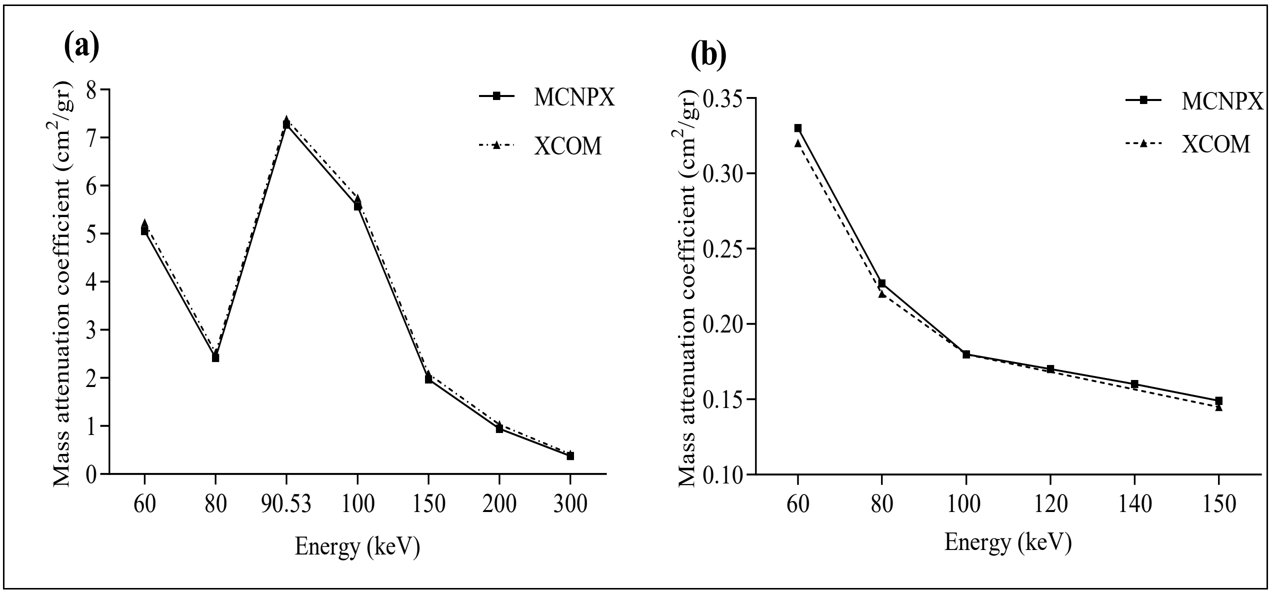


**Figure 2.** Comparison of mass attenuation coefficients of pure silicon shielding (a) and pure bismuth (b) at different energies obtained with the MCNP Monte Carlo code and Xcom standard data.

## 3.2 Mass Attenuation Coefficients of Phosphate Glass

In this section, the mass attenuation coefficients were calculated for twelve glass protectors containing varying percentages of bismuth oxide and lead, based on MC simulation data. Independent of material density, these coefficients are provided in figures for eight photon energies: 50, 60, 80, 100, 120, 140, 150, and 200 keV.

### 3.2.1 Lead Added Phosphate Glasses

The attenuation coefficients of lead-added phosphate glass with varying weight percentages (PZPb10, PZPb20, PZPb30, PZPb40, and PZPb50) at photon energies relevant to diagnostic radiology are presented in Figure 3. The data show a strong correlation between the simulation results and the Xcom standard database, indicating the reliability of the findings. Additionally, as the photon beam energy increases, there is a noticeable decrease in the radiation attenuation capability of the simulated glasses. As shown in Figure 3, the attenuation coefficients of Pb-doped phosphate glass samples decrease with increasing photon energy. The results confirm that higher Pb concentrations lead to better attenuation, particularly at lower energies.

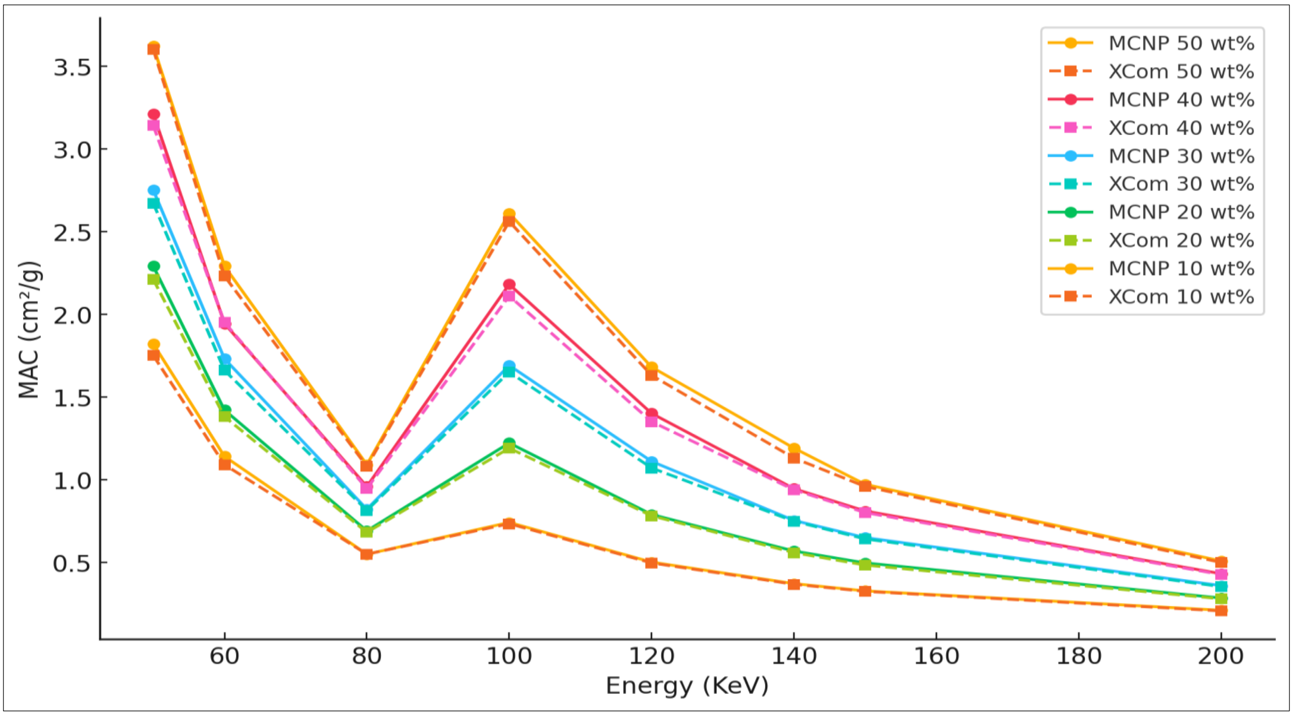


**Figure 3.** Mass attenuation coefficients of lead (Pb) added-phosphate glass PZPb10, PZPb20, PZPb30, PZPb40 and PZPb50 in the energies used in diagnostic radiology

### 3.2.2 Bismuth Added Phosphate Glasses

The attenuation coefficients of Bi added phosphate glass with varying weight percentages (PZBi10, PZBi20, PZBi30, PZBi40, and PZBi50) at photon energies pertinent to medical imaging applications are presented in Figure 4. Similarly, the data presented a robust correlation between the simulation results and the XCOM standard database, demonstrating the dependability of the findings. Furthermore, as expected, as the photon beam energy increases, there is a noticeable decrease in the radiation attenuation capability of the simulated glasses.

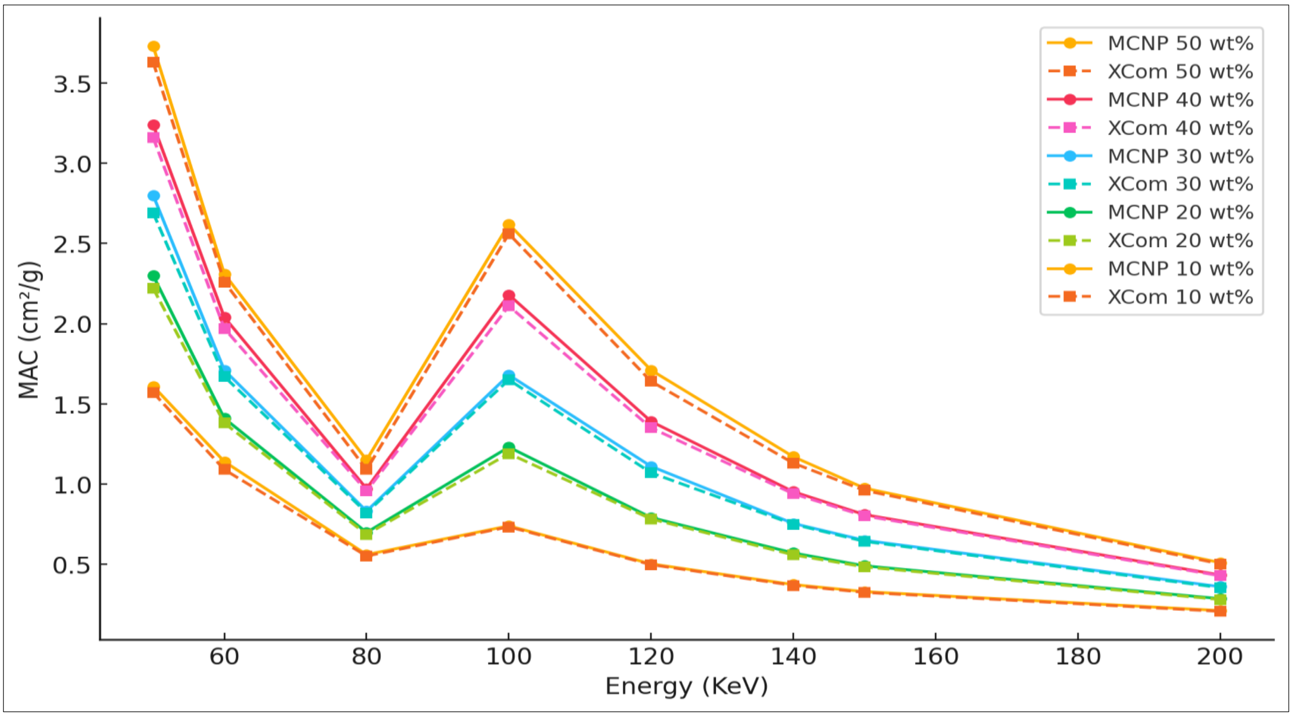


**Figure 4.** Mass attenuation coefficients of bismuth (Bi) added-phosphate glass PZBi10, PZBi20, PZBi30, PZBi40, and PZBi50 in the energies used in diagnostic radiology.

In this study, we developed and assessed the radiation shielding properties of glass doped with NPs of Bi and Pb to be used in radiology by an MCNP simulator. We compared the results with the data from the XCOM standard database. Figures 3 and 4 show that the attenuation coefficients of phosphate shields containing Pb and Bi fillers indicate that Bi shields are slightly more efficient than lead glass shields. For instance, at a constant concentration of 50%, Bi and Pb NPs exhibit mass attenuation coefficients of 1.15 and 1.09, respectively, at an energy of 80 keV. At a constant concentration of 40% by weight, the mass attenuation coefficients for Bi and Pb NPs are 0.971 and 0.958 at the same energy level. For a constant concentration of 30% by weight, the mass attenuation coefficients are 0.831 for Bi and 0.821 for Pb at the same photon energy. At a concentration of 20% by weight, the coefficients are 0.698 for Bi and 0.690 for Pb, respectively. For a weight percentage of 10%, these values are 0.560 for Bi and 0.549 for Pb. These results demonstrated that Bi fillers have superior attenuation capabilities compared to lead fillers, particularly at higher concentrations and lower energies. This enhanced attenuation can be attributed to the photoelectric effect, as Bi has a higher atomic number than lead, leading to more effective interactions with radiation.

In a related study by Karimi et al. [17], different glass shields were evaluated and compared against international standards. The study included one commercially available lead-based shield, four newly investigated shielding materials, four recently analyzed shields, and three new lead-free alternatives. The shielding factors for these materials were calculated, introducing three types of glass made from borate, phosphate, and silicate compounds, designated as Ir1, Ir2, and Ir3. Additionally, mass attenuation coefficients for all shields were obtained from the XCOM database, specifically within the diagnostic X-ray energy range of 40–120 keV. Ultimately, they found that Ir3 glasses emerged as the recommended lead-free transparent shielding materials within photon energies relevant to diagnostic imaging. In a study by Zakaly et al. [18], the influence of BaO incorporation on the optical, structural, mechanical stability, and nuclear radiation shielding properties of barium borosilicate glasses was examined. The linear attenuation coefficients for the glasses labeled Ba00, Ba05, Ba10, Ba20, and Ba30 were measured at energies of 81 keV and 2614 keV, yielding values of 0.4951, 1.0129, 1.5780, 2.8795, and 4.4203 at 81 keV, and 0.1030, 0.1084, 0.1148, 0.1278, and 0.1397 at 2614 keV, respectively. These results were compared with data from the XCOM program and the FLUKA MC simulation code across photon energies ranging from 81 to 2614 keV, and their findings are in line with our results.

In another study by Elsafi et al. [19], the influence of $Bi_2O_3$ concentration and particle size on the properties of $Bi_2O_3$ glass was assessed. The compositions examined included $SiO_2$- $Bi_2O_3$-CaO-MgO- $Bi_2O_3$ -$K_2O$-$Na_2O$-ZnO. The research compared plain glass with samples containing 10% bulk $Bi_2O_3$ NPs, 10% $Bi_2O_3$ NPs, 20% bulk $Bi_2O_3$, and 20% NPs. Results indicated that higher $Bi_2O_3$ content enhanced shielding effectiveness, with NPs demonstrating superior attenuation compared to bulk $Bi_2O_3$ at equivalent concentrations. Further analysis of the half-value layer showed that glasses with $Bi_2O_3$ NPs could attenuate the same photon levels at reduced thickness, highlighting the efficacy of NP shields. Our findings are in concordance with those reported by Karimi et al., who also observed improved shielding in phosphate-based glasses. However, our results emphasize the advantage of nanoparticle incorporation, which was less pronounced in their study. Similarly, compared to Elsafi et al. [19], our Bi2O3 nanoparticle-doped glasses showed higher attenuation at equivalent concentrations, likely due to optimized glass composition and particle size distribution.

## 4. Conclusion

This study tested the effect of adding two elements, lead and bismuth, to make X-ray shielding glass in phosphate glass. According to the figure of attenuation coefficients in shields, it was observed that $\mu/\rho$ decreases with the increase of beam energy. The mass attenuation coefficient at 50 keV energy is much higher than at other energies in all shields. $\mu/\rho$ decreases sharply when more energy is increased. Therefore, the lowest $\mu/\rho$ in all six shields is 200 keV energy. The observed jumps in attenuation coefficients around 90 keV and 92 keV are due to the K-absorption edges of Bi and Pb, respectively, where a sharp increase in photoelectric absorption occurs owing to the sudden availability of inner shell electrons for interaction. This phenomenon is attributed to the photon energy reaching the binding energy of the K-shell electrons in these elements. When this threshold is exceeded, the probability of photoelectric interaction rises significantly, leading to a peak in the mass attenuation coefficient ($\mu/\rho$). Since bismuth and lead have high atomic numbers and strong electron binding energies, these materials' edge effect becomes highly pronounced.

The occurrence of the attenuation coefficient peak can be seen at the absorption edges if it is calculated, but in some shields, the increase of $\mu/\rho$ in the first energy after the absorption edge is also seen. For example, in shields containing bismuth oxide, $\mu/\rho$ is higher at 100 keV energy than at 80 keV energy, which is caused by the bismuth absorption edge effect. In some other shields, this mutation of the mass attenuation coefficient has occurred after the absorption edge of that metal, such as the effect caused by the lead absorption edge in lead shields at 80 kiloelectron volts energy. Because their absorption edges and as a result the $\mu/\rho$ jump occur at lower energies, which is not visible due to the larger $\mu/\rho$ and lack of calculation for the absorption edges, the increase in $\mu/\rho$ is not visible at the first energy after that. At lower energies, the main cause of beam attenuation is photoelectric reaction. So that at energies of 50 keV, the dominant interaction in the shields is photoelectric. With the increase in energy, the contribution of Compton scattering in the interaction of photons with matter increases, and as a result, the attenuation coefficient decreases. Bi-doped phosphate glass's attenuation performance was superior to that of Pb-doped glass at all comparable weight concentrations, particularly in the diagnostic X-ray energy range. This can be attributed to the higher atomic number of bismuths, which enhances photoelectric interactions at lower photon energies.

## Author Contributions

They all read and approved the final version of the paper. The first author: Contributed to manuscript writing and critical review, performed language editing, and assisted in preparing figures and tables. The second author: Supervision and project administration; conducted the MCNP simulations, drafted the manuscript, prepared figures and tables, and provided overall oversight and guidance throughout the study.

## Conflicts of Interest

All the authors declare no conflict of interest.

## Ethical Review and Approval

Ethical approval was not required for this research.

## References

[1] T. Srivastava, E. Chirikova, S. Birk, F. Xiong, T. Benzouak, J. Y. Liu, P. J. Villeneuve, L. B. Zablotska, *Exposure to ionizing radiation and risk of dementia: A systematic review and meta-analysis,* Radiation Research 199 (5) (2023) 490–505.

[2] N. Hamada, *Cancer and non-cancer effects following ionizing irradiation*, Cancers 16 (6) 1141 (2024) 1-5.

[3] E. Mansouri, A. Mesbahi, R. Malekzadeh, A. Mansouri, *Shielding characteristics of nanocomposites for protection against X- and gamma rays in medical applications: Effect of particle size, photon energy, and nano-particle concentration*, Radiat Environ Biophys 59 (4) (2020) 583–600.

[4] P. Mehnati, R. Malekzadeh, M. Y. Sooteh, *Use of bismuth shield for protection of superficial radiosensitive organs in patients undergoing computed tomography: A literature review and meta-analysis*, Radiol Phys and Technol 12 (1) (2019) 6–25.

[5] M. Kılıç, M. Çağlar, Y. Karabul, Z. Güven Özdemir, O. İçelli, *Dielectric and gamma shielding properties of sodium silicate glassy structure modified with tungsten*, Radiation Effects and Defects in Solids 174 (3–4) (2019) 229–247.

[6] P. Mehnati, R. Malekzadeh, M. Y. Sooteh, *Application of personal non-lead nano-composite shields for radiation protection in diagnostic radiology: A systematic review and meta-analysis*, Nanomedicine Journal 7 (3) (2020) 170–182.

[7] R. Malekzadeh, V. S. Zali, O. Jahanbakhsh, M. Okutan, A. Mesbahi, *The preparation and characterization of silicon-based composites doped with $BaSO_4$, $WO_3$, and PbO nanoparticles for shielding applications in PET and nuclear medicine facilities*, Nanomedicine Journal 7 (4) (2020) 324–334.

[8] S. Niksarlioglu, F. Akman, M. E. Pekdemir, S. Y. Kuzu, M. R. Kaçal, M. Yılmaz, *An extensive investigation on gamma shielding properties of PLA/$Gd_2O_3$ nanocomposites*, Radiation Physics and Chemistry 208 (2023) 110936.

[9] H. B. Kavanoz, Ö. Akcali, O. Toker, B. Bilmez, M. Çağlar, O. İçelli, *A novel comprehensive utilization of vanadium slag/epoxy resin/antimony trioxide ternary composite as gamma ray shielding material by MCNP 6.2 and BXCOM*, Radiation Physics and Chemistry 165 (2019) 108446.

[10] M. Çağlar, Y. Karabul, M. Kılıç, Z. G. Özdemir, O. İçelli, *$Na_2Si_3O_7$/Ag micro and nano-structured glassy composites: The experimental and MCNP simulation surveys of their radiation shielding performances*, Progress in Nuclear Energy 139 (2021) 103855.

[11] P. Mehnati, R. Malekzadeh, B. Divband, M. Y. Sooteh, *Assessment of the effect of nano-composite shield on radiation risk prevention to Breast during computed tomography*, Iranian Journal of Radiology 17 (1) (2020) 96002.

[12] M. H. M. Zaid, K. A. Matari, H. A. A Sidek, I. R. Ibrahim, *Bismuth modified gamma radiation shielding properties of titanium vanadium sodium tellurite glasses as a potent transparent radiation-resistant glass applications*, Nuclear Engineering and Technology 53 (4) (2021) 1323–1330.

[13] B. Aygün, E. Şakar, E. Cinan, N. Y. Yorgun, M. I. Sayyed, O. Agar, A. Karabulut, *Development and production of metal oxide doped glasses for gamma ray and fast neutron shielding*, Radiation Physics and Chemistry 174 (2020) 108897.

[14] I. Kebaili, I. Boukhris, M. I. Sayyed, M. B. Tonguc, M. S. Al-Buriahi, *Effect of $TiO_2/V_2O_5$ substitution on the optical and radiation shielding properties of alkali borate glasses: A Monte Carlo investigation*, Ceramics International 46 (16) (2020) 25671–25677.

[15] K. Won-In, N. Sirikulrat, P. Dararutana, *Radiation shielding lead-free glass based on barium-bearing glass using Thailand quartz sands*, Advanced Materials Research 214 (2011) 207–211.

[16] O. Bawazeer, K. Makkawi, Z. B. Aga, H. Albakri, N. Assiri, K. Althagafy, A. Ajlouni, *A review on using nanocomposites as shielding materials against ionizing radiation*, Journal of Umm Al-Qura University for Applied Sciences 9 (2023) 325–340.

[17] M. Karimi, K. Ghazikhanlou-sani, A. R. Mehdizadeh, H. Mostaghimi, *Lead-free transparent shields for diagnostic X-rays: Monte Carlo simulation and measurements*, Radiological Physics and Technology 13 (2020) 276–287.

[18] H. M. H. Zakaly, H. A. Saudi, S. A. M. Issa, M. Rashad, A. I. Elazala, H. O. Tekin, Y. B. Saddek, , *Alteration of optical, structural, mechanical durability and nuclear radiation attenuation properties of barium borosilicate glasses through BaO reinforcement: Experimental and numerical analyses*, Ceramics International 47 (4) (2021) 5587–5596.

[19] M. Elsafi, M. A. El-Nahal, M. I. Sayyed, M. I. Sayyed, I. H. Saleh, M. I. Abbas, *Effect of bulk and nanoparticle $Bi_2O_3$ on attenuation capability of radiation shielding glass*, Ceramics International 47 (14) (2021) 19651–19658.